# A DFT Study of the Adsorption and Dissociation of CO on Sulfur-Precovered Fe(100)

**Daniel Curulla-Ferré,*,† A. Govender,† Tracy C. Bromfield,‡ and J. W. (Hans) Niemantsverdriet†**

*Schuit Institute of Catalysis, Technische Universiteit Eindhoven, P.O. Box 513, 5600 MB Eindhoven, The Netherlands, and Sasol Technology R&D, PO Box 1, Sasolburg 1947, South Africa*

*Received: October 19, 2005; In Final Form: May 15, 2006*

Sulfur is known to be a poison to several catalytic reactions, e.g., the Fischer−Tropsch synthesis (FTS), in which it affects drastically the performance of both iron- and cobalt-based catalysts. However, despite the importance of this industrial process, little is known about what elementary steps are poisoned by sulfur. In the present article, we report, using density functional theory, the effect of sulfur on one of the most relevant reactions in the FTS: the dissociation of carbon monoxide over iron surfaces. We have studied the adsorption and dissociation of CO on Fe(100)−S−p(2 × 2) ($\theta_S$ = 0.25 ML) and on Fe(100)−S−c(2 × 2) ($\theta_S$ = 0.50 ML). We have found surface configurations that correlate well with the desorption features observed in temperature-programmed desorption mass spectroscopy. In addition, we have calculated the activation energy of CO dissociation on Fe(100)−S−p(2 × 2), which, interestingly, is very similar to the activation energy of CO dissociation on the sulfur-free Fe(100) surface. However, the sign of the reaction changes by the presence of sulfur; CO dissociation is highly exothermic on the sulfur-free Fe(100) surface, whereas on the Fe(100)−S−p(2 × 2) surface, it is slightly endothermic. Moreover, according to our results, the influence of sulfur in the CO dissociation seems to be short-ranged.

## Introduction

The Fischer−Tropsch synthesis (FTS) is an attractive route for the production of chemicals and fuels from coal, natural gas, and potentially even biomass sources. The process commences with the production of syngas (either by gasification of coal and biomass sources or by reforming of natural gas), which is then reacted over a suitable catalyst to yield a plethora of products ranging from methane to waxy paraffins, as well as oxygenates. Depending on the feedstock, the formation of various sulfur- and nitrogen-containing compounds is concomitant with the production of syngas. It is imperative that these compounds are effectively removed during the purification of the synthesis gas, because they are widely regarded as catalyst poisons in the FTS. Sulfur is reported to cause a decline in catalyst activity, as well as an increased propensity toward methane formation.[1]

Commercially, syngas is purified via the Rectisol process, which is effective in removing S-containing species down to a level of 5 ppb in syngas. This means that, under normal operation, industrial Fischer−Tropsch catalysts are constantly exposed to low levels of sulfur that may accumulate on the surface of the catalyst, causing gradual poisoning. Indeed, recent DFT studies showed that the activation energy for the dissociation of $H_2S$ on Fe(100)[2] and Fe(110)[3] is very low, and therefore, the presence of $H_2S$ in the feed will lead to the deposition of atomic S on the surface of the catalyst. In the event of a significant sulfur breakthrough, the effect on the catalyst performance could be catastrophic.[1] Given this scenario, it is important to understand the mechanism by which the adsorbed sulfur species affect the most fundamental reaction in the FTS: the dissociation of CO. For this purpose, we have studied the adsorption and dissociation of CO on S-precovered Fe(100) surface using density functional theory; we have chosen the Fe(100) surface because the only experimental study available dealing with the influence of atomic S on the CO dissociation on iron single crystals was actually carried out on the Fe(100) surface.[4]

The Fe(100) surface has been mainly used to model iron catalysts in fundamental studies. Several articles deal with the adsorption and dissociation of CO on clean Fe(100), using a diversity of surface science techniques such as temperature-programmed desorption (TPD),[4−7] electron-energy loss spectroscopy (EELS),[4,6,8] X-ray photoelectron spectroscopy (XPS),[4−6] ultraviolet photoelectron spectroscopy (UPS),[7] X-ray photoelectron diffraction (XPD),[9] and near-edge X-ray absorption fine structure (NEXAFS).[4,10] Despite the moderate number of experimental papers studying the adsorption of CO on iron single crystals, we have found only a few articles studying the adsorption of S on Fe(100)[11,12] or the adsorption of CO on S-precovered Fe(100).[4]

Experiments show that the addition of small amounts of sulfur does not significantly modify the TPD spectrum of CO on Fe(100). As the sulfur coverage is increased, new TPD features develop at 356 and 288 K, whereas the desorption features characteristic of the sulfur-free Fe(100) decrease in intensity. At the saturation coverage of sulfur, only one desorption feature is observed in the TPD spectrum at 183 K. TPD experiments clearly show the poisoning effect of sulfur on the CO dissociation; the desorption feature at 820 K that corresponds to the recombination and desorption of C and O from the surface decreases in intensity as the sulfur coverage is increased and eventually vanishes at sulfur coverages above $^1/_4$ ML. Further, EELS measurements at 340 K show the CO stretching loss at

* To whom correspondence should be addressed. Email: d.curulla.ferre@tue.nl. Fax number: +31402473481.
† Technische Universiteit Eindhoven.
‡ Sasol Technology R&D.

10.1021/jp055979v CCC: $33.50 
Published on Web 06/22/2006

1210 $cm^{-1}$ on sulfur-free surface as well as on the Fe(100) surface precovered with 0.3 ML of sulfur. The fact that the CO stretching frequency did not shift in combination with the fact that new TPD features developed at the expense of those characteristic of the sulfur-free surface was interpreted as that sulfur effects were only short range.

The adsorption and dissociation of CO on Fe(100) has been studied at different theory levels. Nevertheless, the number of theoretical studies is rather scarce.[13−17] Further, there are only a few theoretical articles using different computational methods that have been devoted to the study of the nature of the poisoning effect of sulfur on single-crystals: e.g., on Rh(100) using self-consistent surface linearized augmented plane wave method (SLAPW)[18,19] and also density-functional calculations (DFT),[20] on Rh(111) using DFT,[21] and on Ni(100) using tight-binding extended Hückel calculations[22] and all-electron full-potential linearized augmented plane wave method (FP-LAPW).[23] Feibelman et al.[18,19] showed that the interaction between sulfur and Rh atoms did not involve substantial charge transfer and that the charge associated with the sulfur atom was screened to zero at short distances; thus implying that sulfur effects are only short-range or "steric". However, they showed that sulfur perturbs the local density of states (LDOS) at the Fermi level, concluding that sulfur effects actually are long-range. On the other hand, Zhang et al.[21] concluded that the interaction between CO and sulfur atoms is mainly short range in nature on the basis of the analysis of the chemisorption properties of CO and also on the analysis of LDOS.

In the present article, we report adsorption energies, structures, and vibrational frequencies of CO on S-precovered Fe(100) for several adsorption configurations. We have performed a full analysis of the vibrational frequencies of CO, thus determining what structures are stable adsorption states and also characterizing the transition-state structure for CO dissociation. We have found CO adsorption states that correlate well with the new CO desorption features observed in the TPD spectra of CO on S-precovered Fe(100). In addition, we have calculated the activation energy of dissociation of CO at $^1/_4$ ML as well as at $^1/_2$ ML on the Fe(100)−S−p(2 × 2) surface to quantify the effect of sulfur as well as CO coverage on the dissociation of the CO molecule.

## Computational Details

We have used the Vienna ab initio simulation package (VASP),[24,25] which performs an iterative solution of the Kohn−Sham equations in a plane-wave basis set. Plane-waves with a kinetic energy below or equal to 400 eV have been included in the calculation. The exchange-correlation energy has been calculated within the generalized gradient approximation (GGA) using the form of the functional proposed by Perdew and Wang,[26,27] usually referred to as Perdew−Wang 91 (PW91). The electron−ion interactions for C, O, S, and Fe are described by the projector-augmented wave (PAW) method developed by Blöchl.[28] This is essentially an all-electron frozen-core method combining the accuracy of all-electron methods and the computational simplicity of the pseudopotential approach, especially in the implementation of Kresse and Joubert.[29] A first-order Methfessel−Paxton smearing function with a width of 0.1 eV has been used to account for fractional occupancies.[30] Spin-polarized calculations have been done to account for the magnetic properties of iron. The relative positions of the metal atoms have been fixed initially as those in the bulk, with an optimized lattice parameter of 2.8313 Å (the experimental value is 2.8665 Å).[31] The optimized lattice parameter has been calculated using the smallest unit cell that can be used to model the bulk of iron, and its reciprocal space has been sampled with a (15 × 15 × 15) k-point grid generated automatically using the Monkhorst−Pack method.[32] The calculated magnetic moment of bcc iron at the equilibrium lattice constant is 2.16$\mu_B$, in good agreement with the experimental value of 2.22$\mu_B$ reported in Kittel's book.[33]

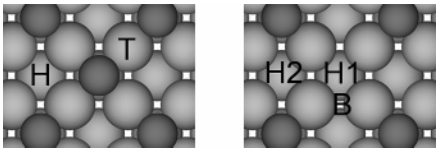


**Figure 1.** Fe(100)−S−c(2 × 2) (Left): CO can adsorb at 4-fold hollow sites (H) and ontop sites (T). Fe(100)−S−p(2 × 2) (Right): CO can adsorb at two distinct 4-fold hollow sites labeled H1 and H2, and at bridge sites (B). Sulfur atoms are represented with dark circles.

The CO molecule has been calculated using a 10 × 10 × 10 $Å^3$ cubic unit cell while for the S, C and O atoms a 10 × 12 × 14 $Å^3$ orthorhombic unit cell has been used. Nonspin polarized calculations for the CO molecule and spin-polarized calculations for the atoms have been done at the Γ point. A Gaussian smearing function with a width of 0.01 eV has been used to account for fractional occupancies.

The Fe(100) surface has been modeled within the slab model approximation using a four-metal layer slab model representing a p(2 × 2) unit cell and six vacuum layers (∼10 Å). The reciprocal space of the p(2 × 2) unit cell has been sampled with a (5 × 5 × 1) k-points grid automatically generated using the Monkhorst−Pack method. Two sulfur coverages have been studied using the same unit cell: Fe(100)−S−p(2 × 2), which contains one sulfur atom per unit cell and corresponds to a sulfur coverage of $^1/_4$ ML, and Fe(100)−S−c(2 × 2), which contains two sulfur atoms per unit cell that corresponds to the sulfur saturation coverage of $^1/_2$ ML (Figure 1). Partial geometry optimizations have been performed including relaxation of the first metal layer, using the RMM-DIIS algorithm.[34] In this method, the forces on the atoms and the stress tensor are used to determine the search directions for finding the equilibrium positions. Geometry optimizations were stopped when all the forces (of the degrees of freedom set in the calculation) were smaller than 0.01 eV/Å. Vibrational frequencies have been calculated within the harmonic approximation. The second-derivative matrix (or Hessian matrix) has been calculated numerically by displacing every atom independently out of its equilibrium position twice (± 0.02 Å); C, O, and S atoms have been displaced twice in all three directions, whereas the Fe atoms of the topmost layer have been displaced only in the *z* direction to account for the adsorbate−metal coupling.[35] Transition-state structures have been found using the climbing-image nudged-elastic-band method (CI−NEB).[36] All transition-state structures have been characterized by calculating the vibrational frequencies.

## Results and Discussion

We have studied the adsorption of carbon monoxide on a S-precovered Fe(100) surface at two different sulfur coverages, $^1/_4$ ML (1 sulfur atom per unit cell in a p(2 × 2) ordered structure) and $^1/_2$ ML (2 sulfur atoms per unit cell in a c(2 × 2) ordered structure) (Figure 1). Dissociation of carbon monoxide has been studied on the Fe(100)−S−p(2 × 2) surface, and the effect of the coverage of carbon monoxide has been investigated by adding a second CO molecule in the model.

**Adsorption of S on Fe(100).** Our calculations show that the only stable adsorption site for atomic sulfur is the 4-fold hollow

**TABLE 1: Adsorption of $^1/_4$ ML of Atomic Sulfur on Fe(100)**

| | This work | | | Jiang and Carter[2] | | |
|---|---|---|---|---|---|---|
| | $\Delta E_{ads}$[a] (eV) | $E_{rel}$[b] (eV) | $z_S$[c] (Å) | $\Delta E_{ads}$ (eV) | $E_{rel}$ (eV) | $z_S$ (Å) |
| top | −4.32 | 1.86 | 2.030 | −4.06 | 1.94 | 1.96 |
| bridge | −5.11 | 1.07 | 1.709 | −4.79 | 1.21 | 1.75 |
| hollow | −6.18 | 0.00 | 1.022 | −6.00 | 0.00 | 1.03 |
| | $\nu_1$[d] | $\nu_2$[d] | $\nu_3$[d] | $\nu_1$ | $\nu_2$ | $\nu_3$ |
| top | 91i | 91i | 475 | 93i | 100i | 378 |
| bridge | 64i | 257 | 365 | 75i | 192 | 317 |
| hollow | 219[e] | 226 | 226 | 225 | 228 | 233 |

[a] $\Delta E_{Ads}$ is the adsorption energy of S in electron-volts. [b] $E_{Rel}$ is the relative adsorption energy with respect to the adsorption at hollow sites. [c] $z_S$ is the height of the S atoms with respect to the surface. [d] $\nu_1$, $\nu_2$ and $\nu_3$ are the sulfur frustrated vibrations in wavenumbers. [e] Fe−S stretching frequency.

site. The distance between the sulfur atom and the surface plane (from now on Fe−S) is 1.022 Å and the Fe−S stretching frequency is 219 $cm^{-1}$ (Table 1). These results agree well with experimental LEED data[12] and semiquantitatively with recent DFT calculations carried out by Jiang and Carter.[2] The discrepancy in the calculated adsorption energies reported in this work and that from Jiang and Carter is mainly due to the fact that we have used the exchange-correlation functional proposed by Perdew and Wang (see computational details), whereas Jiang and Carter used the Perdew−Burke−Ernzerhof exchange-correlation functional (see Supporting Information).

Further, the interaction energy of sulfur at bridge sites and at ontop sites is 1.07 and 1.86 eV less stable than at hollow sites, respectively. The vibrational analysis shows that the adsorption at bridge sites corresponds to a transition state for diffusion between two adjacent 4-fold hollow sites and that ontop sites are second-order saddle points in the Fe(100)−S−p(2 × 2) potential energy surface (PES).

The adsorption of $^1/_2$ ML of sulfur atoms at hollow sites arranged in a c(2 × 2) structure shifts the Fe−S stretching vibration to higher frequencies, most likely as a result of dipole−dipole interactions. The totally symmetric Fe−S stretch at $^1/_2$ ML is calculated to be at 261 $cm^{-1}$.

**Adsorption of CO on Fe(100)−S−c(2 × 2).** There are two likely adsorption sites accessible for CO on an Fe(100) surface containing $^1/_2$ ML of sulfur atoms arranged in a c(2 × 2) structure: top sites and 4-fold hollow sites (Figure 1). The adsorption energy of CO with the C−O molecular axis perpendicular to the surface at both top and 4-fold hollow sites is lowered significantly with respect to the adsorption energies of CO at the same sites on the sulfur-free surface (Table 2). Adsorption at 4-fold hollow sites is more stable than at top sites and has an adsorption energy of −0.45 eV. Our calculations show that CO adsorbs at 4-fold hollow sites, in agreement with Moon et al.,[4] who suggested that CO molecules fill the empty hollow sites of the S−c(2 × 2) overlayer. [The adsorption energy reported by Moon et al.[4] (page 104) is actually 0.6 kcal/mol, which corresponds to 0.03 eV. The disagreement between the value reported by Moon et al. and our calculated adsorption energy of −0.45 eV is likely a typing error. If one assumes a frequency factor of $10^{13}$ $s^{-1}$ (as in ref. 4) and uses the Redhead equation, one obtains an adsorption energy of ∼10.6 kcal/mol, which corresponds to 0.45 eV.] The calculated adsorption energy of −0.45 eV corresponds to a desorption temperature of ∼180 K, after dividing this adsorption energy by a factor of 0.0025 eV/K,[37] in good agreement with the experimental TPD data reported by Moon et al.[4]

**TABLE 2: Adsorption of CO on S-Precovered Fe(100) ($\theta_S$ = $^1/_2$ ML)**

| | $\Delta E_{ads}$[a] (eV) | $d_{CO}$[b] (Å) | $\Delta d_{CO}$[c] (Å) | $z_{CO}$[d] (Å) | $\theta$[e] (deg) | $z_S$[f] (Å) |
|---|---|---|---|---|---|---|
| | | | Clean Fe(100)[13] | | | |
| ontop | −1.90 | 1.178 | 0.036 | 1.769 | 0.0 | − |
| bridge | −1.79 | 1.197 | 0.055 | 1.383 | 0.0 | − |
| hollow | −1.99 | 1.253 | 0.111 | 0.691 | 0.0 | − |
| tilted | −2.56 | 1.320 | 0.178 | 0.629 (1.459) | 51.0 | − |
| | | | S−c(2 × 2)−Fe(100) | | | |
| ontop | −0.30 | 1.168 | 0.026 | 1.784 | 0.0 | 1.007 |
| bridge | − | − | − | − | − | − |
| hollow | −0.45 | 1.234 | 0.092 | 0.811 | 0.0 | 1.003 |
| tilted | − | − | − | − | − | − |

[a] $\Delta E_{Ads}$ Is the adsorption energy of CO in electron-volts. [b] $d_{CO}$ is the CO distance in Angstroms. [c] $\Delta d_{CO}$ is the elongation of the CO distance with respect to the gas-phase CO distance (1.142 Å). [d] $z_{CO}$ is the height of the CO molecule with respect to the surface level (the value in brackets in the last entry is the height of oxygen atom whereas the value outside the brackets is the height of the carbon). [e] $\theta$ is the angle between the surface normal and the CO molecular axis in degrees. [f] $z_S$ is the height of the S atoms with respect to the surface.

**TABLE 3: Adsorption of CO on S-Precovered Fe(100) ($\theta_S$ = $^1/_2$ ML)**

| | ontop | hollow |
|---|---|---|
| $\nu_1$[a] | 50*i* | 222 |
| $\nu_2$ | 118 | 222 |
| $\nu_3$ | 252 | 236 |
| $\nu_4$ | 266 | 250 |
| $\nu_5$ | 379 | 296 |
| $\nu_6$ | 480 | 326 |
| $\nu_7$ | 496 | 326 |
| $\nu_8$ | 1945 | 1500 |
| **ZPE[b] (eV)** | 0.24 | 0.21 |
| **$\Delta E_{ads}$[c] (eV)** | −0.22 | −0.40 |

[a] $\{\nu_k\}$ are the vibrational frequencies in wavenumbers of the chemisorbed CO molecule plus the in-phase and out-of-phase *z*-frustrated translation of sulfur. [b] ZPE is the zero-point energy in electronvolts. [c] $\Delta E_{Ads}$ is the adsorption energy including the zero-point energy correction (the zero point energy of the CO in the gas-phase and the Fe(100)−S−c(2 × 2) equals 0.16 eV).

Further, the metal−CO distance is enlarged whereas the C−O distance is shortened at both sites with respect to the same adsorption configuration on the sulfur-free Fe(100) surface. Vibrational frequency calculations show that only the adsorption at 4-fold hollow sites is a minimum in the PES, whereas the CO molecule adsorbed at top sites presents an imaginary frequency, and consequently, it is a transition state in the PES (Table 3). Further analysis of the normal modes shows that the imaginary frequency of CO at top sites corresponds to a normal mode in which both carbon and oxygen are moving away from the top site in the direction toward the 4-fold hollow site. Therefore, we conclude that the CO at top sites is a transition state for the diffusion of CO from one 4-fold hollow site to another and that the activation energy for diffusion is as low as 0.15 eV.

Our calculations indicate that CO adsorbs at 4-fold hollow sites on the S−c(2 × 2)-Fe(100) surface. However, the vibrational analysis yields a CO stretching frequency of 1500 $cm^{-1}$ for the CO molecule adsorbed at 4-fold hollow sites, clearly smaller than the experimental value of 2050 $cm^{-1}$ reported by Moon et al.[4] Notice that Moon et al. did not discussed the origin of the 2050 $cm^{-1}$ vibrational feature in their paper. Despite the fact that they assume that CO molecules adsorb on 4-fold hollow sites surrounded by 4 sulfur atoms, they did not explicitly ascribed the feature at 2050 $cm^{-1}$ with

such adsorption mode, probably because of the apparent contradiction of having CO molecules adsorbed at hollow sites that show a frequency of vibration similar to those adsorbed at ontop sites.

On the other hand, the CO stretching frequency calculated for the CO molecule adsorbed ontop on the S−c(2 × 2)−Fe(100) surface is 1945 $cm^{-1}$, which is almost 100 $cm^{-1}$ smaller than the experimental value. In addition, our vibrational analysis suggests that ontop sites are not stable minima but maxima on the diffusion coordinate connecting two neighboring hollow sites. All of these results, in combination with the fact that the vibrational spectrum was recorded after saturating the surface with CO at 120 K, lead us to suggest that maybe the reason Moon et al. observed a vibrational frequency of 2050 $cm^{-1}$ could be the presence of multiple layers of CO or the existence of densely packed CO molecules adsorbed at both 4-fold hollow and ontop sites. The presence of multiple layers is not likely because the boiling point of CO is below 120 K; however, we cannot rule out the possibility of filling both 4-fold hollow and ontop sites. Further research needs to be done to address this particular issue. Nevertheless, there is still an open question: presuming that CO molecules adsorb on both ontop and 4-fold hollow sites after CO saturation of the S−c(2 × 2)−Fe(100) surface, why did Moon et al. not observe anything in the region around 1500 $cm^{-1}$? Maybe the reason is that sulfur atoms screen the change in dipole moment of the CO molecules vibrating at 4-fold hollow sites, and consequently, this vibration is less intense and actually vanishes; EELS experiments in the off-specular mode would help to answer to this question.

Further, the Fe−CO stretch is 236 $cm^{-1}$ ($\nu_3$) and the normal mode shows that the Fe−CO stretch is coupled in-phase with the sulfur adlayer. We have obtained two Fe−S stretching modes (because we have two sulfur atoms in the model) that correspond to the totally symmetric and the totally antisymmetric Fe−S stretching vibrations. The totally symmetric Fe−S stretching frequency is 296 $cm^{-1}$ ($\nu_5$), in good agreement with the loss at 290 $cm^{-1}$ reported by Moon et al.[4] On the other hand, the antisymmetric Fe−S stretching frequency is 250 $cm^{-1}$ ($\nu_4$) and has no experimental counterpart because it has zero intensity due to the symmetry.

**Adsorption of CO on Fe(100)−S−p(2 × 2) ($\theta_{CO}$ = 1/4 ML).** Sulfur adsorbs at 4-fold hollow sites and arranges in a p(2 × 2) structure at 1/4 ML. Therefore, CO can adsorb at two distinct 4-fold hollow sites, labeled H1 and H2, and at bridge sites (Figure 1). On the other hand, top sites are blocked by the presence of sulfur. We know from experiments[4,7−9] and also from DFT calculations[13,14] that CO adsorbs on clean Fe(100) at 4-fold hollow sites with the C−O molecular axis tilted away from the surface normal; this adsorption state is referred to in the literature as the CO($\alpha_3$) state and has a desorption temperature of 440 K. Moreover, experiments on S-precovered Fe(100) at sulfur coverages below saturation show a desorption state at 440 K, which indicates that CO molecules still adsorb with a CO($\alpha_3$) orientation (Figure 2).[4]

The adsorption of CO at H1 hollow sites with the CO($\alpha_3$) adsorption-state orientation is only slightly perturbed by the presence of sulfur atoms (Table 4). From now on, we shall refer to this adsorption state as CO($\alpha_3$)′. The adsorption energy of the CO($\alpha_3$)′ is −2.29 eV, which is only 0.25 eV less stable than for the CO($\alpha_3$) state on the sulfur-free surface. Further, we can estimate the interaction between the CO molecule and one sulfur atom, using the pairwise additive potential approximation,[38] to be about 0.06 eV. The influence of the sulfur atoms on the CO adsorption energy is hence very small. Further, the CO distance is shortened only 0.01 Å and the tilting angle is decreased from 51.0° in the CO($\alpha_3$) state in the sulfur-free surface to 48.3° in the CO($\alpha_3$)′ state in the Fe(100)−S−p(2 × 2) surface.

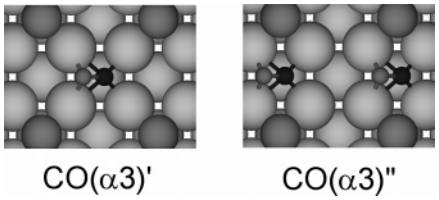


**Figure 2.** Adsorption of CO on the Fe(100)−S−p(2 × 2) surface with a tilted orientation: (Left) CO($\alpha_3$)′ and (Right) CO($\alpha_3$)″ adsorption states. The second CO molecule in the right picture appears as a result of the translational symmetry, so there is only one CO molecule in the unit cell.

**TABLE 4: Adsorption of CO on S-Precovered Fe(100) ($\theta_S$ = 1/4 ML)**

| | $\Delta E_{ads}$[a] (eV) | $d_{CO}$[b] (Å) | $\Delta d_{CO}$[c] (Å) | $z_{CO}$[d] (Å) | $\theta$[e] (deg) | $z_S$[f] (Å) |
|---|---|---|---|---|---|---|
| | | | S−p(2 × 2)-Fe(100) | | | |
| H1 | −1.88 | 1.254 | 0.112 | 0.685 | 0.0 | 0.990 |
| H2 | −1.06 | 1.239 | 0.097 | 0.822 | 0.0 | 0.943 |
| $\alpha_3'$ | −2.29 | 1.311 | 0.169 | 0.648 (1.523) | 48.1 | 1.068 |
| $\alpha_3''$ | −1.55 | 1.315 | 0.173 | 0.654 (1.443) | 53.1 | 1.073 |

[a] $\Delta E_{Ads}$ Is the adsorption energy of CO in electron-volts. [b] $d_{CO}$ is the CO distance in Angstroms. [c] $\Delta d_{CO}$ is the elongation of the CO distance with respect to the gas-phase CO distance (1.142 Å). [d] $z_{CO}$ is the height of the CO molecule with respect to the surface level (the value in brackets in the last entry is the height of oxygen atom whereas the value outside the brackets is the height of the carbon). [e] $\theta$ is the angle between the surface normal and the CO molecular axis in degrees. [f] $z_S$ is the height of the S atoms with respect to the surface.

The adsorption energy of CO at H2 hollow sites in a CO($\alpha_3$) state configuration is −1.55 eV; thus, the adsorption of the CO molecule is 0.74 eV less stable than at H1 hollow sites and 1.00 eV less stable than on the clean surface. We shall refer to this adsorption state as CO($\alpha_3$)″ (Figure 2). The interaction between the CO molecule and one sulfur atom is in this case 0.50 eV, which is considerable. However, the CO distance is not significantly modified, and the tilting angle increases from 51.0° in the CO($\alpha_3$) state in the clean surface to 53.1° in the CO($\alpha_3$)″ state.

We have also calculated the adsorption of CO perpendicular to the surface at the H1 and H2 hollow sites. The adsorption energy of CO at H1 is −1.88 eV, which is 0.11 eV less stable than on the sulfur-free surface. The CO and the Fe−CO distance are not influenced by the presence of the sulfur atoms. On the other hand, the adsorption energy of CO at H2 is −1.06 eV, which is 0.82 eV less stable than at H1 and 0.93 eV less stable with respect to the clean surface. The Fe−CO distance is increased by 0.13 Å and the C−O distance is shortened 0.015 Å. All the calculations that we performed to optimize the CO molecule at bridge sites ended with the CO molecule at hollow sites, either H1 or H2.

The analysis of the vibrational frequencies shows that the CO($\alpha_3$)′ and CO($\alpha_3$)″ adsorption states on the Fe(100)−S−p(2 × 2) surface are minima on the PES (Table 5). On the other hand, the adsorption of CO vertically at H1 hollow sites gives rise to two imaginary frequencies, and consequently, it is not a stable adsorption state but a second-order saddle point in the PES. The normal modes show that these two imaginary frequencies correspond to the rotational motion (along the *x* or the *y* direction) that leads from the vertical to the tilted

**TABLE 5: Adsorption of CO on S-Precovered Fe(100) ($\theta_S$ = 1/4 ML)**

| | H1 | H2 | $\alpha_3'$ | $\alpha_3''$ |
|---|---|---|---|---|
| $\nu$**1** | 175*i* | 194*i* | 210 | 233 |
| $\nu$**2** | 175*i* | 117 | 246 | 256 |
| $\nu$**3** | 233 | 198 | 255 | 315 |
| $\nu$**4** | 237 | 235 | 337 | 320 |
| $\nu$**5** | 237 | 266 | 377 | 388 |
| $\nu$**6** | 276 | 347 | 386 | 497 |
| $\nu$**7** | 1437 | 1487 | 1221 | 1188 |
| **ZPE(eV)** | 0.15 | 0.16 | 0.19 | 0.20 |
| $\Delta E_{ads}$**(eV)** | −1.89 | −1.06 | −2.26 | −1.51 |

[a] Vibrational frequencies are given in wavenumbers. [b] ZPE is the zero-point energy in electronvolts. [c] $\Delta E_{Ads}$ is the adsorption energy including the zero-point energy of the chemisorbed CO and the CO in the gas-phase.

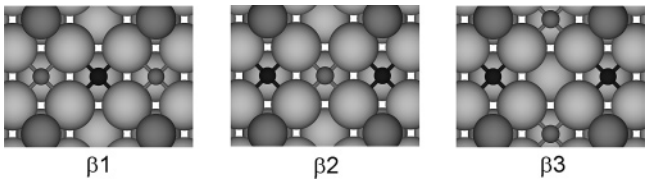


**Figure 3.** Coadsorption of atomic C and atomic O on the Fe(100)−S−p(2 × 2) surface. Small black circles represent atomic C, small gray circles represent atomic O, and large gray circles represent atomic S. (Left) One carbon sits at H2 hollow sites and one oxygen sits at H1 hollow sites (the second oxygen atom plotted in the picture appears by the application of the translational symmetry). (Middle) One carbon sits at H2 hollow sites and one oxygen sites at H1 hollow sites. (Right) Both carbon and oxygen sit at H2 hollows sites and the H1 site is empty.

orientation. The adsorption of CO vertically at H2 hollow sites has one imaginary frequency and therefore it is a first-order saddle point (or a transition state). The normal-mode analysis indicates that this imaginary frequency corresponds to the rotational motion along the *x* direction that leads to the tilted orientation. The fact that we only found one imaginary frequency is understandable because the rotational motion along the *y* direction is hindered by the presence of the sulfur atoms.

The calculated CO stretching frequency of the CO molecule at the CO($\alpha_3$)′ and CO($\alpha_3$)″ adsorption states is 1221 and 1188 cm$^{-1}$, respectively. On the other hand, the calculated CO stretching frequency of the CO molecule at the CO($\alpha_3$) adsorption state on the sulfur-free surface is 1158 cm$^{-1}$; therefore, the CO stretching frequency at the CO($\alpha_3$)′ adsorption state shift upward by 63 cm$^{-1}$ with respect to the stretching frequency of CO on clean surface and only by 30 cm$^{-1}$ in the case of the CO($\alpha_3$)″ adsorption state. Further, calculations yield an Fe−S stretching frequency of about 255 cm$^{-1}$ for both surface configurations. These results agree well with the experimental frequencies reported by Moon et al.[4] at moderate sulfur coverages.

**Dissociation of CO on Fe(100)−S−p(2 × 2) ($\theta_{CO}$ = 1/4 ML).** We shall first show the results obtained for the coadsorption of atomic carbon, oxygen and sulfur. The coadsorption of these three atomic species in our model gives rise to a surface coverage of 0.75 ML. Besides, there are three different configurations in which we can arrange the three atoms on the surface in our model (Figure 3); we have labeled them $\beta_1$, $\beta_2$, and $\beta_3$ (in an attempt to use the same nomenclature as experimentalists, in which the $\beta$ desorption state correspond to the recombination of atomic carbon and oxygen to desorb CO). All three configurations are very similar in stability, and zero-point energy corrections do not change the relative stabilities. In addition, the Fe−S distance is very similar in all three

**TABLE 6: Adsorption Energy and Geometry of the Different Atomic Configurations on Fe(100)−S−p(2 × 2) (This work) and on S-free Fe(100) (Bromfield et al.[13])**

| | This work | | | | Bromfield et al.[13] | | |
|---|---|---|---|---|---|---|---|
| | $\Delta E_{ads}$[a] (eV) | $z_S$[b] (Å) | $z_C$[c] (Å) | $z_O$[d] (Å) | $\Delta E_{ads}$[a] (eV) | $z_C$[c] (Å) | $z_O$[d] (Å) |
| $\beta_1$ | −1.97 | 1.014 | 0.330 | 0.437 | −2.90 | 0.360 | 0.532 |
| $\beta_2$ | −1.99 | 1.000 | 0.212 | 0.488 | | | |
| $\beta_3$ | −2.01 | 1.205 | 0.251 | 0.346 | −3.72 | 0.357 | 0.455 |

a$\Delta E_{Ads}$ is the dissociatively adsorption energy with respect to the CO molecule in the gas-phase. [b] $z_S$ is the height of the S atoms. [c] $z_C$ is the height of the C atoms. [d] $z_O$ is the height of the O atoms.

**TABLE 7: Frustrated Translational Modes along the z-direction for S, C and O in Wavenumbers of the Different Atomic Configurations on Fe(100)−S−p(2 × 2) (see Figure 3)**

| | $\beta_1$ | $\beta_2$ | $\beta_3$ |
|---|---|---|---|
| $\nu_S$ | 235 | 236 | 242 |
| $\nu_S$ | 297 | 321 | 365 |
| $\nu_S$ | 510 | 552 | 545 |
| **ZPE**[a] **(eV)** | 0.16 | 0.18 | 0.17 |
| $\Delta E_{ads}$[b] **(eV)** | −1.98 | −1.98 | −2.00 |

[a] ZPE is the zero-point energy in electronvolts including the frustrated translational modes along the *x* and y directions (not printed in the table). [b] $\Delta E_{Ads}$ is the dissociatively adsorption energy including the zero-point energy with respect to the CO in the gas-phase.

configurations; the same trend is observed for Fe−C and Fe−O distances (Table 6). The Fe−S distance is around 1.0 Å in the $\beta_1$ and $\beta_2$ configurations and 1.2 Å in the $\beta_3$. The enlargement of the Fe−S distance in the $\beta_3$ configuration can be explained because in such configuration, the sulfur atom interacts strongly with both the carbon and the oxygen atoms, which are in very close proximity to the sulfur atom. The Fe−C distance in all three configurations is very short and ranges between 0.2 and 0.3 Å, and the Fe−O distance ranges between 0.3 and 0.5 Å. The vibrational frequencies show that all three configurations are stable adsorption states (Table 7). The Fe−C stretching frequency is above 500 cm$^{-1}$ in all three configurations, the Fe−O stretching frequency is close to or slightly above 300 cm$^{-1}$, and the Fe−S stretching frequency ranges between 230 and 240 cm$^{-1}$.

Once we have discussed the various atomic configurations, we can turn our attention to the dissociation of the CO molecule. We have calculated two reaction channels for the CO dissociation (Figure 4). In the first reaction channel, the CO molecule is initially in the CO($\alpha_3$)′ adsorption state and the final state is the $\beta_1$ atomic configuration, whereas in the second, the CO molecule is initially in the CO($\alpha_3$)″ adsorption state and the final dissociated state is the $\beta_2$ configuration. Remarkably, the transition-state geometry for CO dissociation is very similar in both reaction channels.

The activation energy for the dissociation of CO in the first reaction channel is 1.29 eV, and the total change in energy due to the reaction is 0.32 eV. Interestingly, the activation energy of dissociation on the clean Fe(100) surface is slightly smaller, 1.14 eV. Thus, the presence of the sulfur atoms shifts the barrier 0.15 eV up. Furthermore, the CO dissociation reaction on the clean surface is exothermic with a total change in energy of −0.34 eV.[13] Therefore, sulfur at 1/4 ML only slightly influences the activation barrier of the reaction but strongly influences the total change in energy and actually changes the sign of the reaction. A direct consequence of the effect of sulfur in the product energy level is that recombination of atomic carbon and atomic oxygen is easier on the Fe(100)−S−p(2 × 2) than

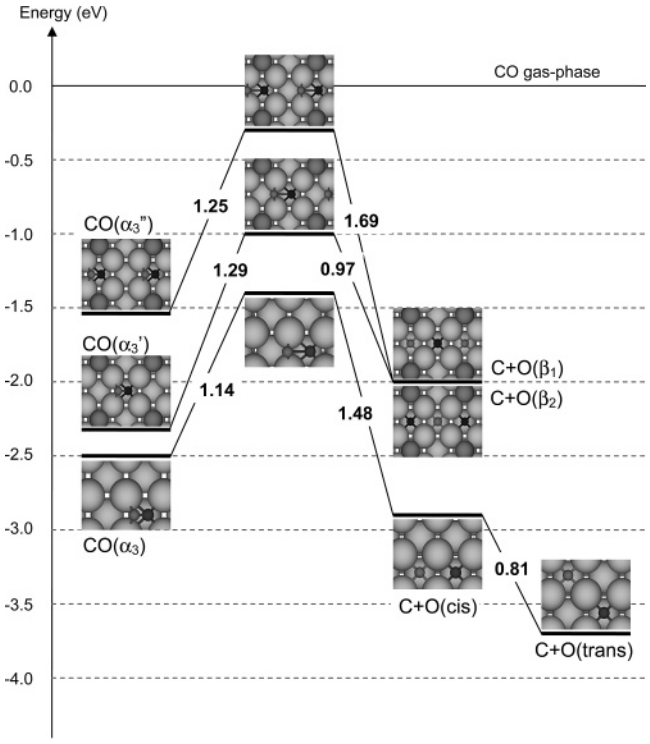


**Figure 4.** Reaction energy diagram of the dissociation of CO on S-precovered Fe(100) ($\theta_S = {}^1/_4$ ML) starting from the CO molecular configurations $\alpha_3'$ and $\alpha_3''$ to yield C + O in the atomic configurations $\beta_1$ and $\beta_2$, respectively. The reaction energy diagram of the dissociation of CO on clean Fe(100) is also presented; data are taken from Bromfield et al.[13] The numbers inserted represent the activation energies of the corresponding elemental steps, expect in the C + O(cis) to C + O(trans), in which it represents the reaction energy.

on the Fe(100) surface, and consequently, sulfur hinders the CO dissociation on Fe(100). We have also calculated the activation energy for C diffusion ($\beta_1 \rightarrow \beta_3$) and O diffusion ($\beta_2 \rightarrow \beta_3$); the activation energy for C diffusion is about 1.30 eV. On the other hand, the activation energy for O diffusion is about 0.62 eV, and it is almost double than that which was calculated on the clean Fe(100) surface (~0.36 eV).[13] Zero-point energy corrections do not significantly change these barriers. An interesting feature is that when oxygen sits almost in a bridge site, when going from $\beta_2 \rightarrow \beta_3$, the normal-mode analysis reveals that this geometry is a stable adsorption site, although the barrier to continue moving to the $\beta_3$ is only 0.11 eV. We already found in a previous work[13] that unlike carbon, which has only one stable adsorption site at 4-fold hollow sites, oxygen has stable adsorption sites at 4-fold hollow as well as at bridge and ontop sites.

The activation energy for CO dissociation in the second reaction channel, in which the CO molecule is initially in the CO($\alpha_3$)$''$ adsorption state, is 1.25 eV, and the total change in energy is −0.44 eV (Figure 4). Both the activation barrier and the total change in energy are very similar to those calculated on the clean surface. Thus, the dissociation of CO is exothermic in the second reaction channel. However, because the relative stability of the two different atomic configurations is very small and the activation barriers in both reaction channels are very similar, the exothermicity of the CO dissociation reaction in the second reaction channel is due to the fact that the CO($\alpha_3$)$''$ adsorption state is less stable than the CO($\alpha_3$)$'$ adsorption state.

**Adsorption of CO on Fe(100)−S−p(2 × 2) ($\theta_{CO} = {}^1/_2$ ML).** We have shown in the discussion above that sulfur has little influence on the CO molecules adsorbed in the CO($\alpha_3$)$'$ state on the Fe(100)−S−p(2 × 2) surface. On the contrary, CO molecules in the CO($\alpha_3$)$''$ adsorption state are strongly influenced by sulfur; the adsorption energy of a CO molecule in the CO($\alpha_3$)$''$ state is 1 eV smaller than in the CO($\alpha_3$) adsorption state on the clean Fe(100) surface. However, the geometry of the chemisorbed CO is only slightly perturbed by the presence of sulfur atoms in both CO($\alpha_3$)$'$ and CO($\alpha_3$)$''$ adsorption states. We can conclude, according to these results, that sulfur influences only the nearest surroundings; that is to say, sulfur effects are short ranged. Moon et al.[4] also concluded that sulfur has short-range effects on the adsorption of CO on Fe(100). They observed that the presence of a small amount of sulfur on the surface did not change the temperature of the desorption states reported on the sulfur-free surface and that with increasing amounts of sulfur, new desorption features developed at 356, 288, and 183 K, whereas those with a counterpart on the sulfur-free surface diminished in intensity and actually vanished at higher sulfur coverages.

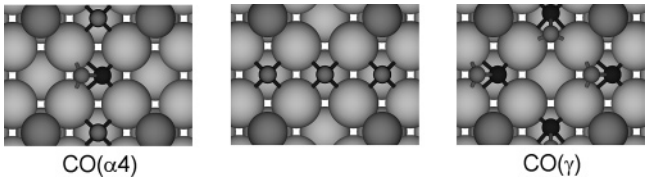


**Figure 5.** Adsorption of ${}^1/_2$ ML of CO on Fe(100)−S−p(2 × 2) surface.

We cannot account for the new desorption features reported by Moon et al. with only one CO molecule in our model. To find out what configurations or adsorption states give rise to these new features reported on the S-precovered Fe(100) surface, we added a second CO molecule in our model, increasing the total surface coverage from ${}^1/_2$ ML to ${}^3/_4$ ML. Therefore, our task is first to determine how many configurations in our model containing one sulfur atom and two CO molecules exist and second, if they are stable adsorption states on the PES.

Starting from the CO($\alpha_3$)$'$ adsorption configuration and adding a second CO molecule, we found two configurations (Figure 5, left and middle). The most stable two-CO molecule configuration has one CO molecule adsorbed in the CO($\alpha_3$)$'$ state and the other CO molecule at an adjacent H2 hollow sites in a vertical orientation; this configuration forms rows of CO molecules on the surface, but it is important to notice that the C−O bond of the CO molecules adsorbed in the CO($\alpha_3$)$'$ state is perpendicular to this row of molecules. The adsorption energy of the vertically adsorbed CO molecule at H2 hollow sites is −0.70 eV, which corresponds to a desorption temperature of 281 K, in good agreement with the TPD desorption feature at 288 K reported by Moon et al.[4] The second two-CO molecule configuration that we found has one CO molecule at H1 hollow sites not in the CO($\alpha_3$)$'$ state geometry but vertically adsorbed, and the other CO molecule is at H2 hollow sites in a vertical orientation as well. The adsorption energy of the second CO molecule adsorbed vertically at H2 hollow sites is −0.81 eV, which corresponds to a desorption temperature of 326 K and might be tentatively associated with the TPD desorption feature at 356 K reported by Moon et al. However, the vibrational analysis shows that only the first configuration found is a minimum in the Fe(100)−S−p(2 × 2)+2CO PES, whereas the second configuration has one imaginary frequency, and therefore, it corresponds to a transition state. We can conclude then that we have found a configuration that explains the new desorption feature at 288 K that appears when CO is adsorbed on sulfur-precovered Fe(100); we shall refer to this configuration

as CO($\alpha_4$). However, we cannot explain at the moment the origin of the other desorption feature at 356 K.

The vibrational analysis of the CO($\alpha_4$) configuration yields a CO stretching frequency of 1246 $cm^{-1}$ for the CO($\alpha_3$)′-like molecule and 1568 $cm^{-1}$ for the vertically adsorbed CO at H2. In addition, the Fe−S stretch has a frequency of 270 $cm^{-1}$ and the Fe−CO stretch of the CO molecule at H2 hollow sites is 231 $cm^{-1}$. These results agree well with the experimental vibrational frequencies reported by Moon et al., who recorded an EELS spectrum of CO on S-precovered Fe(100) at a sulfur coverage of 0.3 ML. In such experiments, Moon et al. observed an energy loss at 1210 $cm^{-1}$ attributed to the CO molecule in a tilted orientation and a loss at 290 $cm^{-1}$ attributed to the Fe−S stretch. Unfortunately, the experimental spectrum was cut at 1500 $cm^{-1}$, and therefore, we have no information about other bands at higher frequencies. In addition, the experimental spectrum was recorded at 340 K, and at such conditions only the CO($\alpha_3$)′ state might be occupied.

If we start from the less stable adsorption configuration with only one CO molecule and one sulfur atom, in which the CO molecule is adsorbed in the CO($\alpha_3$)″ state, we found uniquely one new two-CO molecule configuration that was a stable adsorption state (Figure 5, right). Such configuration has both CO molecules at H2 hollow sites in a CO($\alpha_3$)″ geometry. Interestingly, they are not oriented along the same direction on the surface but in perpendicular directions; this is a clear effect of the presence of the sulfur atom. In this new adsorption configuration, both CO molecules have the same C−O distance and the same tilting angle. Moreover, the adsorption energy of the second CO molecule is −1.40 eV, only 0.15 eV less stable than the first CO molecule, thus showing that the interaction between CO molecules is rather small. The desorption temperature of the second CO molecule would be approximately 560 K. Unfortunately, there is no desorption feature in the experimental TPD around this temperature. Further, the vibrational analysis yields two CO stretching frequencies at 1231 and 1246 $cm^{-1}$; though the two CO molecules are not aligned, but in perpendicular directions on the surface, the corresponding normal modes of these two frequencies show that there is some coupling between the vibrational motion of the two CO molecules. Further, the calculated Fe−S stretching frequency is 259 $cm^{-1}$. We shall refer to this stable configuration as CO($\gamma$); we have not used the greek letter $\alpha$ because, unlike the CO($\alpha_4$) adsorption state, this new adsorption state does not have an experimental counterpart in the TPD spectrum reported by Moon et al.[4]

Two more configurations were found containing two CO molecules and one sulfur atom. However, vibrational analysis showed that none of these two configurations were stable adsorption states. In one of them, the two CO molecules were adsorbed at H1 hollow sites in a perpendicular orientation with respect to the surface plane; in such configuration, the vibrational analysis yields two imaginary frequencies that correspond to the tilting of one CO molecule along the *x* direction and the other one along the *y* direction, ending up in the former configuration described above. In the other configuration, both CO molecules were adsorbed again at H1 hollow sites, but in this case, one CO molecule was perpendicular to the surface and the other one was tilted; the vibrational analysis showed in this case one imaginary frequency corresponding to the tilting of the vertically adsorbed CO molecule. Although we did calculations with several other starting configurations, all the attempts ended in one of five configurations described above.

**Dissociation of CO on Fe(100)−S−p(2 × 2) ($\theta_{CO}$ = ½ ML).** The activation energy for CO dissociation, starting from the CO($\alpha_4$) configuration, is 1.44 eV (0.30 eV larger than that on the sulfur-free surface). The final configuration consists of one CO molecule adsorbed vertically at H2 hollow sites, one carbon atom on the surface at the H1 hollow sites (adjacent to the CO molecule) and one oxygen atom at the remaining H2 hollow sites adjacent to the carbon and to the sulfur atom. The activation energy for dissociation is however, larger than the adsorption energy of the CO molecule vertically adsorbed at H2 hollow sites in the starting configuration. Consequently, one-half of the CO molecules desorb as temperature is increased and the other half of the CO molecules, which are in the CO($\alpha_3$)′ state, dissociate following the first reaction channel discussed previously (see Figure 4).

On the other hand, the activation energy for dissociation starting from the CO($\gamma$) configuration is about 1.71 eV. The final configuration consist in one CO molecule adsorbed like in the CO($\alpha_3$)″ adsorption-state, one carbon atom in the other H2 hollow site and one oxygen atom in the H1 hollow site. In such configuration, the oxygen atoms at H1 hollow site and the CO molecules at the H2 hollow sites form a row. The adsorption energy of the CO molecule in this configuration is −0.23 eV. Therefore, the dissociation channel for CO dissociation starting from the CO($\gamma$) configuration is a concerted-process in which half of the CO molecules dissociate and the other half desorb from the surface. However, the activation energy for dissociation from the CO($\gamma$) configuration is larger than the adsorption energy of the *second* CO molecule (−1.40 eV) in the same adsorption state, and therefore, it is most likely that half of the CO molecules desorb before this reaction channel can occur. At the same time, the remaining CO molecules will dissociate, because the activation energy of dissociation of the CO($\alpha_3$)″ state is about 1.25 eV, and consequently, a concerted reaction would be likely to happen. However, this mechanism is very unlikely to happen because the CO($\gamma$) configuration does not have a counterpart in the TPD spectrum, as we discussed above.

## Conclusions

We have calculated several surface configurations containing one or two sulfur atoms in the unit cell and one or two CO molecules; these calculations permits us to establish a relation between the TPD desorption features reported for CO on sulfur-precovered Fe(100) with actual microscopic configurations, as for instance the desorption features at 183 and 288 K. However, there are still a few features not resolved in the TPD spectrum; larger unit cells should be used to try to find the microscopic configurations responsible for these features. Moreover, we have shown that the influence of sulfur on the chemisorption geometry of CO, e.g., CO($\alpha_3$)′ and CO($\alpha_3$)″, is very little. The CO stretching frequency shifts slightly to higher wavenumbers, but the effect of sulfur on the vibrational frequencies is very small as well. In addition, the influence of sulfur on the adsorption energy of the CO molecule with the surface is only considerable at short distances; the adsorption energy of CO($\alpha_3$)′ is only slightly lowered, whereas the adsorption energy of CO($\alpha_3$)″ drops 1 eV with respect to the adsorption energy of CO($\alpha_3$) on the sulfur-free surface. All of our calculations, then, support the idea that the interaction between CO and S on Fe(100) is short ranged, at least with respect to the adsorption energies.

Concerning the reactivity, our calculations show that the activation energy for CO dissociation does not increase signifi-

cantly. Actually, the difference between the activation energy for dissociation on the Fe(100)−S−p(2 × 2) and the sulfur-free Fe(100) surface is only 0.15 eV. However, sulfur does influence the CO dissociation by changing the sign of the reaction: the CO dissociation (elementary step) is exothermic on the sulfur-free Fe(100) with a reaction energy of −0.34 eV, whereas the dissociation on the Fe(100)−S−p(2 × 2) is endothermic with a reaction energy of +0.32 eV. Moreover, diffusion of either oxygen or carbon does not change the energetics of the reaction on the Fe(100)−S−p(2 × 2) surface any further, due to the fact that all atomic configurations are equally stable. On the other hand, the diffusion of oxygen (after the dissociation step) on the sulfur-free surface is highly exothermic with a reaction energy of −0.82 eV. Therefore, whereas the total reaction energy of CO dissociation on Fe(100)−S−p(2 × 2) is +0.32 eV, it is −1.14 eV on the sulfur-free surface (Figure 4). Accordingly, sulfur clearly hinders the CO dissociation. These results also seem to indicate that sulfur influences the CO adsorption and dissociation on Fe(100) electronically, by changing the relative energy of the reactants, products, and transition-states levels, as well as sterically, by blocking the diffusion of oxygen on the surface, which is mostly responsible for the large exothermicity of the CO dissociation reaction at $^1/_4$ ML on the sulfur-free Fe(100).

**Acknowledgment.** We thank The Netherland Organization for Scientific Research (NWO) for funding this project and the Stichting Nationale Computerfaciliteiten (NCF) for granting us with supercomputational time at SARA in Amsterdam. D.C. acknowledges support through NWO VENI Grant 700-53-403.

## References and Notes

(1) Kritzinger, J. A. *Catal. Today* **2002**, *71*, 307.
(2) Jiang, D. E.; Carter, E. A. *J. Phys. Chem. B* **2004**, *108*, 19140.
(3) Jiang, D. E.; Carter, E. A. *Surf. Sci.* **2005**, *583*, 60.
(4) Moon, D. W.; Bernasek, S. L.; Lu, J. P.; Gland, J. L.; Dwyer, D. J. *Surf. Sci.* **1987**, *184*, 90.
(5) Nassir, M. H.; Frühberger, B.; Dwyer, D. J. *Surf. Sci.* **1994**, *312*, 115.
(6) Lu, J.-P.; Albert, M. R.; Bernasek, S. L. *J. Phys. Chem.* **1990**, *94*, 6028.
(7) Cameron, S. D.; Dwyer, D. J. *Langmuir* **1988**, *4*, 282.
(8) Moon, D. W.; Bernasek, S. L.; Dwyer, D. J.; Gland, J. L. *J. Am. Chem. Soc.* **1985**, *107*, 4363
(9) Saiki, R. S.; Herman, G. S.; Yamada, M.; Osterwalder, J.; Fadely, C. S. *Phys. Rev. Lett.* **1989**, *63*, 283.
(10) Dwyer, D. J.; Rausenberger, B.; Lu, J.-P.; Bernasek, S. L.; Fischer, D. A.; Cameron, S. D.; Parker, D. H.; Gland, J. L. *Surf. Sci.* **1989**, *224*, 375.
(11) Rhodin, T. N.; Brucker, C. F. *Solid State Commun.* **1977**, *23*, 275.
(12) Legg, K. O.; Jona, F.; Jepsen, D. W.; Marcus, P. M. *Surf. Sci.* **1977**, *66*, 25.
(13) Bromfield, T. C.; Curulla Ferré, D.; Niemantsverdriet, J. W. *ChemPhysChem* **2005**, *6*, 251.
(14) Sorescu, D. C.; Thompson, D. L.; Hurley, M. M.; Chabalowski, C. F. *Phys. Rev. B: Condens. Matter Mater. Phys.* **2002**, *66*, 035416.
(15) Mehandru, S. P.; Anderson, A. B. *Surf. Sci.* **1988**, *201*, 345.
(16) Blyholder, G.; Lawless, M. *Surf. Sci.* **1993**, *290*, 155.
(17) Meehan, T. E.; Head, J. D. *Surf. Sci.* **1991**, *243*, L55.
(18) Feibelman, P. J.; Haman, D. R. *Phys. Rev. Lett.* **1984**, *52*, 61.
(19) Feibelman, P. J.; Haman, D. R. *Surf. Sci.* **1985**, *149*, 48.
(20) Nieskens, D. L. S.; Curulla Ferré, D.; Niemantsverdriet, J. W. *ChemPhysChem* **2005**, *7*, 1293.
(21) Zhang, C. J.; Hu, P.; Lee, M.-H. *Surf. Sci.* **1999**, *432*, 305.
(22) Zonnevylle, M. C.; Hoffmann, R. *Langmuir* **1987**, *3*, 452.
(23) Wimmer, E.; Fu, C. L.; Freeman, A. J. *Phys. Rev. Lett.* **1985**, *55*, 2618.
(24) Kresse, G.; Hafner, J. *Phys. Rev. B: Condens. Matter Mater. Phys.* **1993**, *47*, 558.
(25) Kresse, G.; Furthmüller, J. *Phys. Rev B: Condens. Matter Mater. Phys.* **1991**, *44*, 13298.
(26) Perdew, J. P.; Chevary, J. A.; Vosko, S. H.; Jackson, K. A.; Pederson, M. R.; Singh, D. J.; Fiolhais, C. *Phys. Rev. B: Condens. Matter Mater. Phys.* **1992**, *46*, 6671.
(27) Wang, Y.; Perdew, J. P. *Phys. Rev. B: Condens. Matter Mater. Phys.* **1991**, *44*, 13298.
(28) Blöchl, P. E. *Phys. Rev. B: Condens. Matter Mater. Phys.* **1994**, *50*, 17953
(29) Kresse, G.; Joubert, J. *Phys. Rev. B: Condens. Matter Mater. Phys.* **1999**, *59*, 1758.
(30) Methfessel, M.; Paxton, A. T. *Phys. Rev. B: Condens. Matter Mater. Phys.* **1989**, *40*, 3616.
(31) Kohlhaas, R.; Donner, P.; Schmitz-Pranghe, N. *Z. Angew. Phys.* **1967**, *23*, 245. See also www.webelements.com.
(32) Monkhorst, H. J.; Pack, J. D. *Phys. Rev. B: Condens. Matter Mater. Phys.* **1972**, *13*, 5188.
(33) Kittel, C. In *Introduction to Solid State Physics*, 7th ed.; John Wiley and Sons: New York, 1996; p 449.
(34) Pulay, P. *Chem. Phys. Lett.* **1980**, *73*, 393.
(35) Head, J. D. *Int. J. Quantum Chem.* **1997**, *65*, 827.
(36) Henkelmann, G.; Uberuaga, B. P.; Jónsson, H. *J. Chem. Phys.* **2000**, *113*, 9901.
(37) Knor, Z. *Surf. Sci.* **1985**, *154*, L233.
(38) Curulla Ferré, D.; Van Bavel, A. P.; Niemantsverdriet, J. W. *ChemPhysChem* **2005**, *6*, 450.